Sphingomyelins suppress the targeted disruption of lysosomes/endosomes by the photosensitizer NPe6 during photodynamic therapy

Joseph A. CARUSO, Patricia A. MATHIEU and John J. REINERS, Jr[1]

Institute of Environmental Health Sciences, Wayne State University, Detroit, MI 48201, U.S.A.

Recent studies have described a biochemical pathway whereby lysosome disruption and the released proteases initiate the intrinsic apoptotic pathway. Irradiation of murine hepatoma 1c1c7 cells preloaded with the lysosomal photosensitizer NPe6 (*N*-aspartyl chlorin e6) caused a rapid loss of Acridine Orange staining of acidic organelles, release of cathepsin D from late endosomes/lysosomes and the activation of procaspase-3. Pretreatment of NPe6-loaded cultures with 10–50 μM 3-*O*-MeSM (3-*O*-methylsphingomyelin) caused a concentration-dependent suppression of apoptosis following irradiation. This suppression reflected a stabilization of lysosomes/endosomes, as opposed to an inhibition of the accumulation of photosensitizer in these organelles. Exogenously added sphingomyelin, at comparable concentrations, offered some protection, but less than 3-*O*-MeSM. Fluorescence microscopy showed that 3-*O*-MeSM competed with NBD-C$_6$-sphingomyelin (6-{[*N*-(7-nitrobenz-2-oxa-1,3-diazol-4-yl)-amino]hexanoyl} sphingosyl phosphocholine) for co-localization with LysoTracker Red in acidic organelles. Pre-treatment of 1c1c7 cultures with 3-*O*-MeSM also suppressed the induction of apoptosis by TNFα (tumour necrosis factor α), but offered no protection against HA14-1 [ethyl 2-amino-6-bromo-4-(1-cyano-2-ethoxy-2-oxoethyl)-4H-chromene-3-carboxylate], staurosporine, tunicamycin or thapsigargin. These results suggest that exogenously added 3-*O*-MeSM is trafficked to and stabilizes late endosomes/lysosomes against oxidant-induced damage, and further implicate a role for lysosomal proteases in the apoptotic processes initiated by TNFα and lysosomal photosensitizers.

Key words: apoptosis, cathepsin D, lysosome, NPe6, 3-*O*-methylsphingomyelin, photodynamic therapy, procaspase, tumour necrosis factor α (TNFα).

INTRODUCTION

The endosomal/lysosomal system consists of a complex and dynamic set of cytosolic compartments that are involved in the turnover of cellular proteins, down-regulation and recycling of cell-surface receptors and lipid components, release of recycled nutrients, destruction of pathogenic organisms and antigen processing [1–3]. Lysosomes are the main storage vesicles for acidic hydrolases and proteases. It is thought that protein degradation occurs when lysosomes fuse with late endosomes or autophagic vacuoles and release all or part of their contents.

The membrane structure enclosing lysosomes and late endosomes creates an environment suitable for storage and activation of resident degradative enzymes, and protects the cell from unwanted autoproteolysis. Cell death can occur if the integrity of the endolysosomal membrane is compromised. Indeed, the proapoptotic effects of many agents are related to their abilities to cause the release/translocation of endolysosomal proteases to the cytosol. Examples of such agents include reactive oxygen species [4–6], generators of reactive oxygen species [4,7,8], sphingosine [9,10], α-tocopheryl succinate [11], amyloid β-peptide [12] and TNFα (tumour necrosis factor α) [10,13,14].

Diverse experimental approaches have implicated lysosomal proteases in the initiation of apoptosis. In the case of TNFα, several investigators have reported that the cytokine stimulates the release/translocation of lysosomal proteases into the cytosol [10,13]. The induction of apoptosis by TNFα has been suppressed by pharmacological and molecular modulation of lyso-

some/endosome function or stability [15,16], by the induction of lysosome exocytosis before cytokine exposure [16] and by pre-incubation of cultures with inhibitors of the lysosomal protease cathepsin B [17]. Furthermore, cathepsin B null mice and cells derived from such mice are resistant to the cytotoxic effects of TNFα [13,17]. The abilities of extracts of purified endosomes/lysosomes [8,18,19] and purified cathepsins [20] to convert Bid into tBid provide a plausible mechanism whereby lysosomal/endosomal disruption could lead to the release of cytochrome *c* and activation of the intrinsic apoptotic pathway.

Pharmacological and molecular approaches for inhibition of sphingomyelinases and ceramidases (enzymes involved in the generation of ceramide and its conversion into sphingosine) suppress TNFα-mediated lysosomal damage and apoptosis in several models [21–23]. The bases for these effects are not known, but may relate to the putative detergent properties of sphingosine [9,10]. We recently found that pre-treatment of murine hepatoma 1c1c7 cells with 3-*O*-MeSM (3-*O*-methylsphingomyelin), a putative inhibitor of neutral sphingomyelinase [24], potently suppressed TNFα-induced apoptosis. However, an inability to obtain comparable effects with a different neutral sphingomyelinase inhibitor suggested that 3-*O*-MeSM might mediate its antiapoptotic effects via another mechanism. Accordingly, we examined the possibility that 3-*O*-MeSM may affect the stability of lysosomes/endosomes. As a test model, we examined the effects of 3-*O*-MeSM in a PDT (photodynamic therapy) protocol involving the photosensitizer NPe6 (*N*-aspartyl chlorin e6). We previously reported that NPe6 co-localizes exclusively to a

subpopulation of LysoTracker-stained acidic organelles in cultures of murine hepatoma 1c1c7 cells [8]. In PDT, light-activated photosensitizers generate a pulse of singlet oxygen in the immediate vicinity of the activated sensitizer [25]. Indeed, irradiation of NPe6-sensitized 1c1c7 cultures leads to the rapid loss of AO (Acridine Orange)-stained acidic organelles, release of lysosomal proteases and the chronologically ordered (i) cleavage of Bid, (ii) release of cytochrome c and (iii) activation of procaspase-9 and -3 [8,19,26]. The present study indicates that exogenous 3-O-MeSM is trafficked to acidic organelles and prevents their disruption and induction of apoptosis in NPe6/PDT. Furthermore, pre-treatment with 3-O-MeSM also suppressed the induction of apoptosis in 1c1c7 cultures by TNFα, another putative disruptor of endosomes/lysosomes. However, the sphingolipid did not prevent the induction of apoptosis by agents that do not target and disrupt acidic organelles.

EXPERIMENTAL

Reagents

The fluorescent molecules AO, LTR (LysoTracker Red), HO33342 and NBD-SM (6-{[N-(7-nitrobenz-2-oxa-1,3-diazol-4-yl)amino]hexanoyl} sphingosyl phosphocholine or NBD-C_6-sphingomyelin) were purchased from Molecular Probes (Eugene, OR, U.S.A.). Ac-DEVD-AMC (acetyl-Asp-Glu-Val-Asp-AMC, where AMC stands for 7-amino-4-methylcoumarin) was obtained from BD Biosciences (San Diego, CA, U.S.A.). AMC, GW4869 and recombinant human TNFα were purchased from Calbiochem (La Jolla, CA, U.S.A.). HA14-1 [ethyl 2-amino-6-bromo-4-(1-cyano-2-ethoxy-2-oxoethyl)-^{4}H-chromene-3-carboxylate] was purchased from Ryan Scientific (Isle of Palms, SC, U.S.A.). Rabbit polyclonal anti-caspase 3 was from Santa Cruz Biotechnology (Santa Cruz, CA, U.S.A.). Bicinchoninic acid, CHX (cycloheximide), desipramine, poly(L-lysine), staurosporine, thapsigargin, tunicamycin and SM (from bovine brain) were purchased from Sigma–Aldrich (St. Louis, MO, U.S.A.). NPe6 was a gift from Light Sciences (Issaquah, WA, U.S.A.). 3-O-MeSM was obtained from Biomol (Plymouth Meeting, PA, U.S.A.).

Cell culture

Murine hepatoma Hepa 1c1c7 cells were obtained from Dr J. P. Whitlock, Jr (Stanford University, Stanford, CA, U.S.A.). Adherent cultures were established in either commercially obtained culture dishes or on poly(L-lysine)-coated coverslips. Cells were grown in α-MEM (α-minimal essential medium) supplemented with 5 % (v/v) fetal bovine serum and antibiotics in a 5 % CO_2 atmosphere, at 37 °C. Cultures were plated at densities ensuring exponential growth for at least 3 days. The medium was changed 2 days after plating. Treatments were performed on day 3 of culture.

PDT

Subconfluent cultures were washed twice with PBS before being re-fed with the complete medium containing NPe6. After a 60 min loading period, the cultures were washed three times with PBS, re-fed and then irradiated. Cultures were irradiated for 10–80 s at room temperature (24 °C) using a 600 W quartz-halogen lamp with IR radiation attenuated by a 10 cm layer of water and an 850 nm cut-off filter. The bandwidth was further confined to 650–700 nm by a broadband interference filter. Light intensity at wavelengths of NPe6 absorbance was 1.5 mW/cm^2. Hence, 1 s of irradiation corresponds to 1.5 mJ/cm^2.

NPe6 loading analyses

The method employed for the measurement of cell-associated NPe6 is similar to a recently published procedure [19]. Subconfluent monolayers grown in 35 mm culture dishes were washed thrice with PBS and re-fed with complete medium containing 11, 22 or 33 μM NPe6. After 60 min, the cultures were washed three times with PBS and flooded with 1.5 ml of water containing 0.5 % Triton X-100. The cultures were scraped 5–10 min later with a rubber policeman and lysates were transferred to conical tubes. Plates were washed once with an additional 1.5 ml of the Triton X-100 solution, and the washes were added to the original lysates. Parallel plates were treated with trypsin/EDTA, and cell numbers were determined with a haemocytometer. NPe6 contents were determined by analysis of the fluorescence signature of NPe6. Specifically, lysates were excited at 400 nm and fluorescence emission was determined with an Instaspec IV CCD (charge-coupled-device) camera (Oriel, Stratford, CT, U.S.A.) coupled with a monochronometer. The CCD was set for a 0.5 s scan in single scan mode. Emission spectra were read at their peaks ($\sim$ 660 nm) and recorded in FU (fluorescence units). The 0.5 % Triton X-100 solution was used to establish a baseline. NPe6 content per cell is expressed as FU/10^3 cells.

DEVDase assay

Procaspase-3 and -7 activations were analysed by monitoring the generation of AMC from the caspase substrate Ac-DEVD-AMC. The procedures used for the harvesting of cells and measuring DEVDase activity have been described in detail in [19]. Changes in fluorescence over time were converted into pmol of product by comparison with a standard curve made with AMC. DEVDase-specific activities are reported as nmol of product $\cdot$ min^{-1} $\cdot$ mg protein^{-1}. The bicinchoninic acid assay, using BSA as a standard, was used to estimate protein concentrations.

Western-blot analyses

The reagents and procedures used for the preparation and processing of cell lysates, SDS gel electrophoresis and immuno-detection of caspase 3 have been described in detail in [19].

Immunofluorescence detection of cathepsin D

Cultures grown on poly(L-lysine)-coated coverslips were washed three times with PBS and fixed in 4 % (w/v) paraformaldehyde/PBS solution for 30 min. Thereafter, the fixed cells were washed three times with PBS and permeabilized with methanol for 5 min on ice. After washing (3× PBS), non-specific autofluorescence was quenched with 100 mM glycine/PBS for 30 min. Subsequently, three washes were carried out with PBS/0.1 % saponin. The coverslips were washed and incubated with blocking buffer (5 % BSA/PBS/0.1 % saponin) for 1 h at 37 °C to block non-specific immunoglobulin binding. The coverslips were washed and incubated with a 1:20 dilution of rabbit anti-human cathepsin D antibody (Oncogene Research Products, San Diego, CA, U.S.A.) and a 1:1000 dilution of the 1D4B rat anti-mouse Lamp-1 antibody (Development Studies Hybridoma Bank, Department of Biological Sciences, University of Iowa) in blocking buffer for 2 h at 37 °C. After washing, secondary detection consisted of 1:200 dilutions of AlexaFluor 488 goat anti-rabbit IgG and AlexaFluor 546 goat anti-rat IgG (Molecular Probes) in blocking buffer for 1 h at 37 °C. Coverslips were washed and incubated for 5 min at room temperature with 500 nM HO33342/PBS. After a final wash, the coverslips were inverted on to glass slips coated with SlowFade solution (Molecular Probes) and sealed with acrylic nail polish. Digital images were
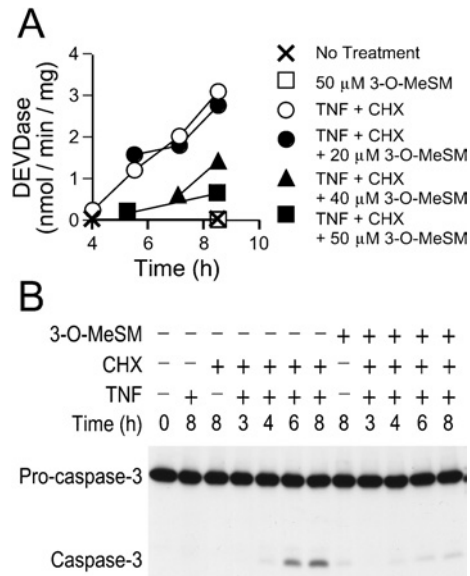
Figure 1   Suppression of TNFα-mediated apoptosis by 3-*O*-MeSM

1c1c7 cultures were pretreated with various concentrations of 3-*O*-MeSM before the addition of 0.5 μg/ml CHX and 30 ng/ml TNFα. 3-*O*-MeSM and CHX were added 60 and 30 min before adding TNFα respectively. In some studies, cultures were treated with only CHX or TNF or 3-*O*-MeSM. Treatments are mentioned in the Figure. Cultures were harvested for subsequent analyses of DEVDase activities (**A**) and Western-blot analyses of procaspase-3 cleavage (**B**) at various time points after the addition of TNFα. (**A**) Results shown are means ± S.D. for three determinations. Similar results were obtained in a second independent experiment. (**B**) Western-blot analyses employed 25 μg of protein per lane.

captured using an Axioplan 2 Imaging Microscope equipped with an ApoTome optical sectioning device (Carl Zeiss, Cologne, Germany).

Fluorescence microscopy of non-fixed cultures

Cultures growing in 35 mm tissue culture dishes were exposed to 100 nM LysoTracker Red. After 30 min, the cultures were treated with 5 μM NBD-SM. At this time, some cultures were concurrently treated with various concentrations of 3-*O*-MeSM. After 20 min of incubation, 500 nM HO33342 was added to the culture medium. After an additional 10 min of incubation, the cultures were washed three times with the medium and the cultures were imaged. All incubations were performed under routine cell-culture conditions (37 °C, 5 % CO$_2$ and α-MEM + 5 % fetal bovine serum). The filter cubes employed for fluorescence microscopy utilized exciter/emitter/beam splitter wavelengths of 500/535/515 nm for NBD-SM, 365/420/395 nm for HO33342 and 515/590/580 nm for LTR.

In PDT studies, approx. 50 min after irradiation, cultures were incubated simultaneously with 500 nM HO33342 and 500 nM AO for 10 min before being sequentially imaged using filter cubes that captured red (AO in an acidic pH environment), green (AO in a neutral pH environment) and blue (HO33342) fluorescence. The filter cubes used for capture of red and green AO fluorescence employed exciter/emitter/beam splitter wavelengths of 365/420/395 nm and 500/535/515 nm respectively. Digital images were captured with an Axiovert 200M fluorescence microscope (Carl Zeiss). The black and white images generated during the capture of AO red fluorescence were inverted in order to quantify AO-stained acidic organelles. Following inversion, backgrounds appeared white, cells appeared light grey and lysosomes/endosomes stood out as discrete black dots.
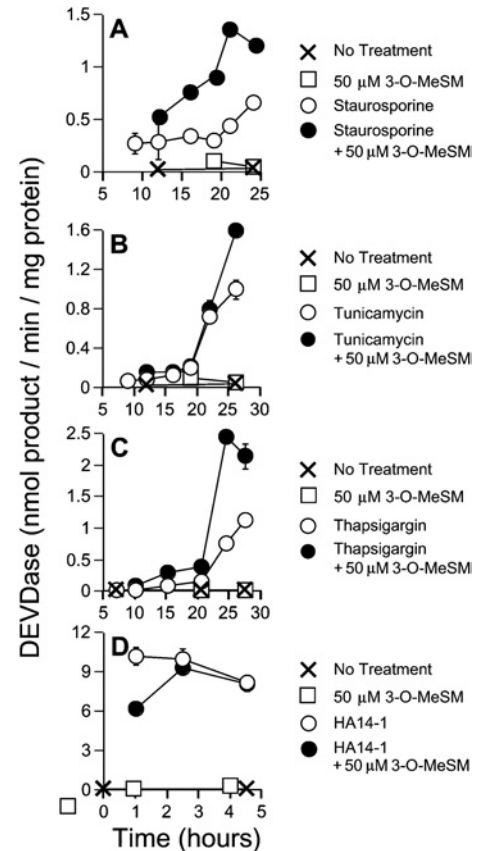

Figure 2   Antiapoptotic property of 3-*O*-MeSM is agent-specific

1c1c7 cultures were treated with 50 μM 3-*O*-MeSM for 30 min before the addition of 300 nM staurosporine (**A**), 3 μg/ml tunicamycin (**B**), 2 μM thapsigargin (**C**) or 25 μM HA14-1 (**D**). Cultures were harvested for subsequent analyses of DEVDase activities at various times after the addition of apoptotic inducer. Specific treatments are noted in the Figure. (**A**–**D**) Results shown are means ± S.D. for three determinations. In all cases, similar results were obtained in a second independent experiment.

Statistical analyses

Data were analysed by one-way ANOVA and Tukey's Multiple Comparison Test (Prism, GraphPad Software, San Diego, CA, U.S.A.). Differences between/among groups were scored as statistically significant if $P < 0.05$.

RESULTS

Selective suppression of apoptosis by 3-*O*-MeSM

Co-treatment of 1c1c7 cultures with TNFα and CHX induced morphological changes consistent with the development of apoptosis (results not shown), and the activation of procaspase-3 and -7, as monitored by measurement of DEVDase activity (Figure 1A). Elevations in DEVDase activity correlated with procaspase-3 processing, as determined by Western-blot analyses (Figure 1B). Co-treatment with 3-*O*-MeSM suppressed the activation of DEVDase in TNFα + CHX-treated cultures in a concentration-dependent fashion. Whereas 20 μM concentration affected neither the kinetics nor the magnitude of DEVDase activation, significant suppression was achieved with 50 μM 3-*O*-MeSM (Figure 1A). Reductions in DEVDase activities were mirrored by decreases in the processing of procaspase-3 (Figure 1B). By itself, 3-*O*-MeSM did not activate DEVDase or the processing of procaspase-3 (Figures 1A and 1B).
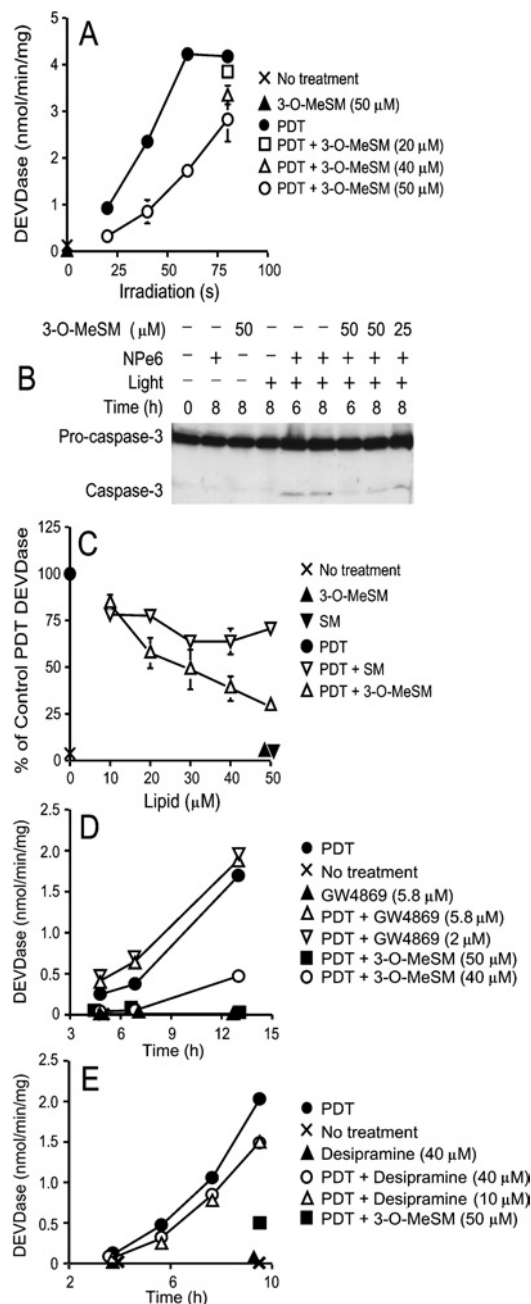
Figure 3   Suppression of PDT-induced procaspase activation by 3-*O*-MeSM, SM and sphingomyelinase inhibitors

(**A**) 1c1c7 cultures were simultaneously treated with 33 μM NPe6 and 3-*O*-MeSM before being washed and irradiated for various lengths of time. Some cultures received only 3-*O*-MeSM. Cultures were harvested 8 h after irradiation for analysis of DEVDase activities. (**B**) 1c1c7 cultures were simultaneously treated with 33 μM NPe6 and 3-*O*-MeSM before being washed and irradiated for 60 s. Some cultures received only 3-*O*-MeSM, NPe6 or light. Cultures were harvested 6 or 8 h after irradiation for analysis of caspase 3 by Western blotting. Analyses employed 25 μg of protein/lane. (**C**) 1c1c7 cultures were simultaneously treated with 33 μM NPe6 and various concentrations of 3-*O*-MeSM or SM for 60 min before being washed and irradiated for 40 s. Cultures were harvested 8 h after irradiation for analysis of DEVDase activities. (**D**) 1c1c7 cultures were treated with GW4869 or 3-*O*-MeSM for 2.5 h and with 33 μM NPe6 for 90 min before being washed and irradiated for 60 s. GW4869 was re-added to the cultures immediately after irradiation. Cultures were harvested at various times after irradiation for analysis of DEVDase. (**E**) 1c1c7 cultures were treated with desipramine for 3.5 h and with 3-*O*-MeSM or 33 μM NPe6 for 90 min before being washed and irradiated for 60 s. Cultures were harvested at various times after irradiation for analysis of DEVDase. Specific treatments are noted in each panel. Results shown are means $\pm$ S.D. for triplicate analyses. Results similar to those depicted in (**A**, **C**–**E**) were obtained in a second independent experiment.
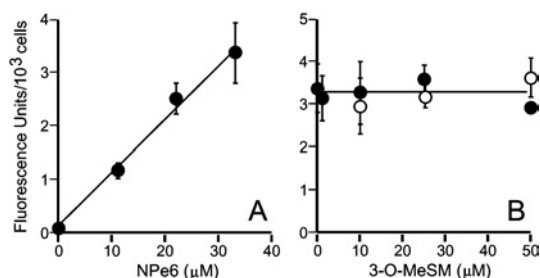
Figure 4   NPe6 loading in the presence of 3-*O*-MeSM

(**A**) 1c1c7 cultures were treated with increasing concentrations of NPe6 (●) for 1 h before being harvested for analysis of NPe6 contents. (**B**) 1c1c7 cultures were simultaneously treated with 33 μM NPe6 + 3-*O*-MeSM (●) for 1 h before being harvested for analysis of NPe6 contents. Alternatively, cultures were loaded with NPe6 for 1 h and various concentrations of 3-*O*-MeSM for 30 min (○), before processing. (**A**, **B**) Results shown are means $\pm$ S.D. for analyses performed on four culture dishes. Similar results were obtained in a second independent study.

The antiapoptotic effects of 3-*O*-MeSM did not carry over to other chemical inducers of apoptosis. In the case of staurosporine, co-treatment with 50 μM 3-*O*-MeSM elevated and accelerated the appearance of DEVDase activities (Figure 2A). Similarly, DEVDase activities in tunicamycin (Figure 2B) and thapsigargin (Figure 2C)-treated cultures were elevated by co-treatment with 3-*O*-MeSM. Finally, although 50 μM 3-*O*-MeSM moderately retarded the initial activation of DEVDase by the non-peptidic Bcl-2 antagonist HA14-1, comparable DEVDase activities were ultimately reached within a very short period of time (Figure 2D). Indeed, every cell was shrunken and decorated with apoptotic blebs within 3 h of HA14-1 treatment, irrespective of treatment (results not shown).

Effects of 3-*O*-MeSM on PDT-induced procaspase activation

Several studies have implicated a role for neutral sphingomyelinase in the initiation of the proapoptotic effects of TNFα [21,23]. Concentrations of 3-*O*-MeSM having antiapoptotic effects in our TNFα studies have been reported by others to inhibit neutral sphingomyelinase activity [24,27]. However, attempts to duplicate the protective effects of 3-*O*-MeSM with G4869, a recently described inhibitor of neutral sphingomyelinase [23], were unsuccessful (results not shown). Consequently, we entertained the possibility that 3-*O*-MeSM may mediate its protective effects by modulating lysosome/endosome stability.

Irradiation of 1c1c7 cultures preloaded with 33 μM of the lysosomal photosensitizer NPe6 activated DEVDase in a light dose-dependent manner (Figure 3A). Co-treatment of NPe6-sensitized cultures with 50 μM 3-*O*-MeSM inhibited DEVDase activation following irradiation (Figure 3A), and the processing of pro-caspase-3 (Figure 3B). Suppression was light dose-dependent and maximal at the lower light doses. The degree of suppression was also dependent on 3-*O*-MeSM concentration. Specifically, DEVDase specific activities progressively decreased as 3-*O*-MeSM concentrations increased over the range 10–50 μM. This concentration dependence was seen following irradiation for either 80 s (Figure 3A) or 40 s (Figure 3C).

3-*O*-MeSM is structurally similar to SM with the exception of the substitution of a methoxy group for a hydroxy group on C-3. Co-treatment of NPe6-sensitized 1c1c7 cultures with various concentrations of SM before irradiation had moderate effects on DEVDase activities after irradiation (Figure 3C). PDT-induced DEVDase activities were suppressed approx. 25–30 % by
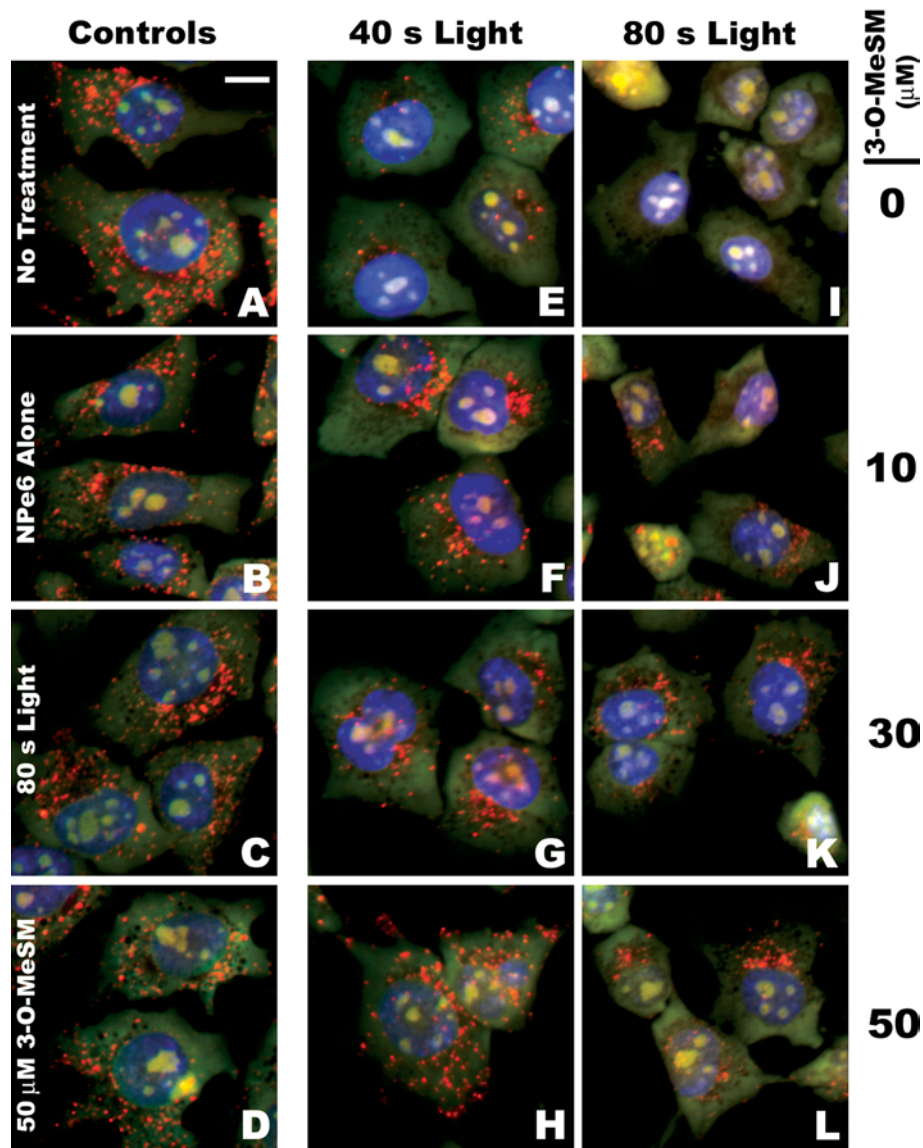
Figure 5   3-*O*-MeSM suppression of PDT-induced acidic organelle disruption

1c1c7 cultures were left untreated or treated with 33 μM NPe6, light or NPe6 + light in the absence or presence of various concentrations of 3-*O*-MeSM. Some cultures were incubated with NPe6 and/or 3-*O*-MeSM for 1 h and 30 min respectively before being washed, re-fed and irradiated. Approximately 30 min after irradiation, cultures were loaded with AO and HO33342 and imaged 10 min later. (**A**) Untreated cultures, (**B**) cultures treated with NPe6, (**C**) 80 s of light, (**D**) 50 μM 3-*O*-MeSM, (**E–H**) NPe6 + 40 s of light $\pm$ various concentrations of 3-*O*-MeSM and (**I–L**) NPe6 + 80 s of light $\pm$ various concentrations of 3-*O*-MeSM. (**A**) Scale bar, 10 μm.

co-treatment with SM. However, unlike what was observed with 3-*O*-MeSM, the suppressive effect of SM did not dramatically change at concentrations above 10 μM SM (Figure 3C).

Co-treatment of cultures with concentrations of GW4869 sufficient to completely inhibit neutral sphingomyelinase *in vitro*, and just below the threshold of insolubility in our culture media ($\sim$6 μM), did not prevent PDT-induced apoptosis (Figure 3D). Similarly, pretreatment of cultures with concentrations of desipramine reported to rapidly reduce acidic sphingomyelinase activities in several cell types [28–30] offered minimal protection in the PDT protocol (Figure 3E). Hence, it seemed unlikely that the protective effects of 3-*O*-MeSM in our PDT protocol reflected its functioning as a putative modulator/inhibitor of neutral or acidic sphingomyelinases.

Effects of 3-*O*-MeSM on cellular NPe6 contents

We previously demonstrated that the proapoptotic effects of NPe6 in PDT are related to the concentration of NPe6 used for sensitization [19]. We also showed that meaningful comparisons of different cell lines in NPe6 PDT require that analyses be made with cells having comparable NPe6 loads [19]. Hence, the issue arose as to whether the effects of 3-*O*-MeSM in our PDT model reflected alterations in NPe6 loading. Figure 4(A) shows that NPe6 cellular contents were proportional to sensitizer concentration over the range 0–33 μM. Simultaneous co-treatment of cultures with 33 μM NPe6 and 1–50 μM 3-*O*-MeSM did not affect NPe6 loading (Figure 4B). Similarly, co-treatment of cultures with 3-*O*-MeSM during the final 30 min of NPe6 sensitization (total
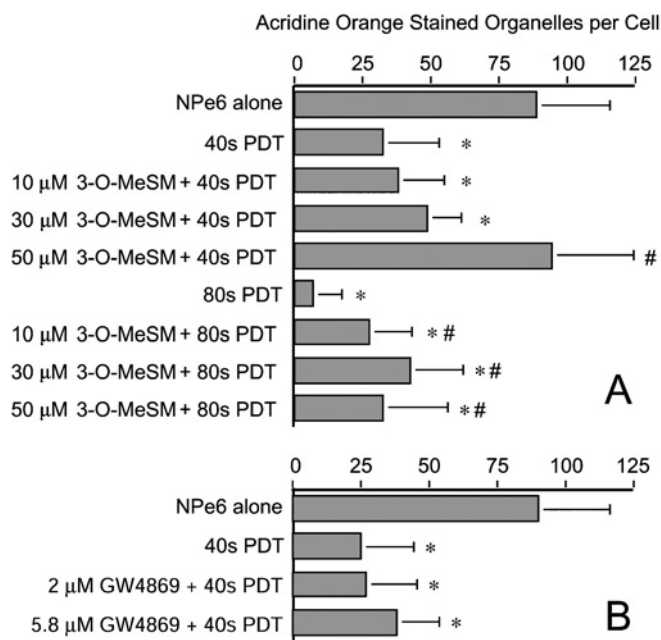
Acridine Orange Stained Organelles per Cell

Figure 6   Quantification of AO-stained organelles

(**A**) 1c1c7 cultures were treated and processed as described in Figure 5. (**B**) 1c1c7 cultures were left untreated or treated with GW4869 for 2.5 h and/or 33 μM NPe6 for 90 min before being washed and irradiated for 40 s. Approximately 30 min after irradiation, cultures were loaded with AO and HO33342, and imaged 10 min later. Digital images were subsequently analysed for the number of AO-stained acidic organelles per cell. (**A**, **B**) Results shown are means $\pm$ S.D. for analyses performed on 25–60 cells per treatment group and are from independent experiments. *$P < 0.05$, significantly less than NPe6 alone group; #$P < 0.05$, significantly greater than the corresponding PDT treatment group.

sensitization time was 60 min) did not affect NPe6 loading (Figure 4B). Hence, the reduced DEVDase activities observed in NPe6 PDT were not the consequence of alterations in NPe6 loading.

3-O-MeSM suppression of PDT-induced acidic organelle breakage

AO-stained acid organelles in 1c1c7 cultures exhibited a punctate pattern (Figure 5A). This pattern was not particularly affected by a 1 h preincubation with 33 μM NPe6 (Figure 5B), 80 s of irradiation (Figure 5C) or preincubation with 50 μM 3-O-MeSM (Figure 5D). However, AO staining was dramatically decreased in cultures sensitized with 33 μM NPe6 and irradiated for 40 s (Figure 5E), and further reduced in sensitized cultures that had been irradiated for 80 s (Figure 5I). Analyses of 25–35 individual cells that had been sensitized with 33 μM NPe6 indicated that irradiation for 40 or 80 s reduced the number of AO-stained organelles per cell by ~67% and ~92% respectively (Figure 6A).

Co-treatment of NPe6-sensitized cultures with 3-O-MeSM prevented irradiation-induced loss of AO staining (Figures 5F–5H and 5J–5L). Quantification of AO-stained organelles in individual cells demonstrated that the protective effect was concentration-dependent over the range 10–50 μM in cultures irradiated for 40 s (Figure 6A). Indeed, co-treatment with 50 μM 3-O-MeSM completely prevented the loss of AO-stained organelles in NPe6-sensitized cultures irradiated for 40 s. Protection also occurred in NPe6-sensitized cultures irradiated for 80 s (Figure 6A). However, in agreement with the DEVDase data presented in Figure 3(A), the degree of protection mediated by 50 μM 3-O-MeSM was lower in cultures treated with the higher light dose (Figure 6A). In contrast, co-treatment of cultures with GW4869, which offered no protection against the induction of PDT-induced apoptosis

(Figure 3D), did not prevent PDT-induced loss of AO-stained organelles (Figure 6B).

As a complement to the above studies, we also monitored the staining patterns of the lysosomal/endosomal membrane protein Lamp-1 [1] and the luminal protease cathepsin D by indirect immunofluorescence microscopy (Figure 7). In 1c1c7 cultures, both cathepsin D and Lamp-1 exhibited punctate staining (Figures 7A and 7B respectively). The appearance of orange/yellow staining following overlay of images taken from the same z plane scan suggests co-localization of the two proteins (Figure 7C). Following irradiation of NPe6-sensitized cultures, there was a decrease in the cathepsin D signal, but not the Lamp-1 signal, relative to what was observed in control cultures (compare Figures 7A versus 7D and Figures 7B versus 7E respectively). A less subjective analysis is facilitated by overlay of the cathepsin D (green) and Lamp-1 (red) images. Specifically, whereas there is a little red signal seen in the control group (Figure 7C), red is dominant in the scans of cultures having undergone PDT (Figure 7F). Such a change is consistent with the loss of cathepsin D from Lamp-1-positive lysosomes/endosomes.

Co-treatment of cultures with 3-O-MeSM and NPe6, in the absence of light, had little effect on the co-localization of cathepsin D and Lamp-1 (compare Figures 7A versus 7I). However, loss of cathepsin D staining in NPe6-sensitized cultures after PDT could be prevented by pre-treatment with 3-O-MeSM. Specifically, cathepsin D fluorescence intensities were greater in PDT groups pre-treated with 50 μM 3-O-MeSM (compare Figures 7D versus 7J). 3-O-MeSM-mediated protection is also suggested by the loss of red staining and the reappearance of yellow/orange staining (compare Figures 7F and 7L), which could only occur if Lamp-1 and cathepsin D co-localized.

Exogenously added NBD-SM is taken up by endocytosis and initially found in early endosomal/sorting vesicles [31–33]. Thereafter, depending on cell type, it is transported to either the Golgi or late endosomes/lysosomes [31–33]. NBD-SM-stained 1c1c7 cultures exhibited a punctate pattern that was similar to the pattern obtained with LTR (Figures 8A and 8B). Overlay of the two images confirmed that the two fluorescent probes co-localized in some vesicles/organelles (Figure 8C). This co-localization was eliminated if NBD-SM and 3-O-MeSM were added within seconds of one another to cultures preloaded with LTR (Figures 8D–8L). Furthermore, the competition by 3-O-MeSM with NBD-SM for sites co-stained by LTR was concentration-dependent (Figures 8F and 8L).

DISCUSSION

The present study demonstrates that preincubation with 3-O-MeSM suppresses the development of apoptosis in NPe6-sensitized 1c1c7 cultures after light activation of the photosensitizer. These effects were paralleled by a suppression of PDT-induced acidic organelle disruption. We previously used this model to demonstrate how a targeted disruption of acidic organelles could initiate the intrinsic apoptotic pathway via proteolytic activation of Bid [8]. A major strength of the model is its specificity. Fluorescence microscopy indicates that virtually all NPe6 fluorescence in 1c1c7 cultures localizes to organelles that are co-stained by LysoTracker Blue [8]. Whereas cathepsin B is released from acidic organelles within minutes of irradiating NPe6-sensitized 1c1c7 cultures [26], parallel releases of mitochondria-derived cytochrome c and ER (endoplasmic reticulum)-derived Ca^{2+} do not occur [8,34]. Other criteria also support the conclusion that NPe6 does not target mitochondria or the ER. Specifically, we and others have demonstrated that mitochondrial and
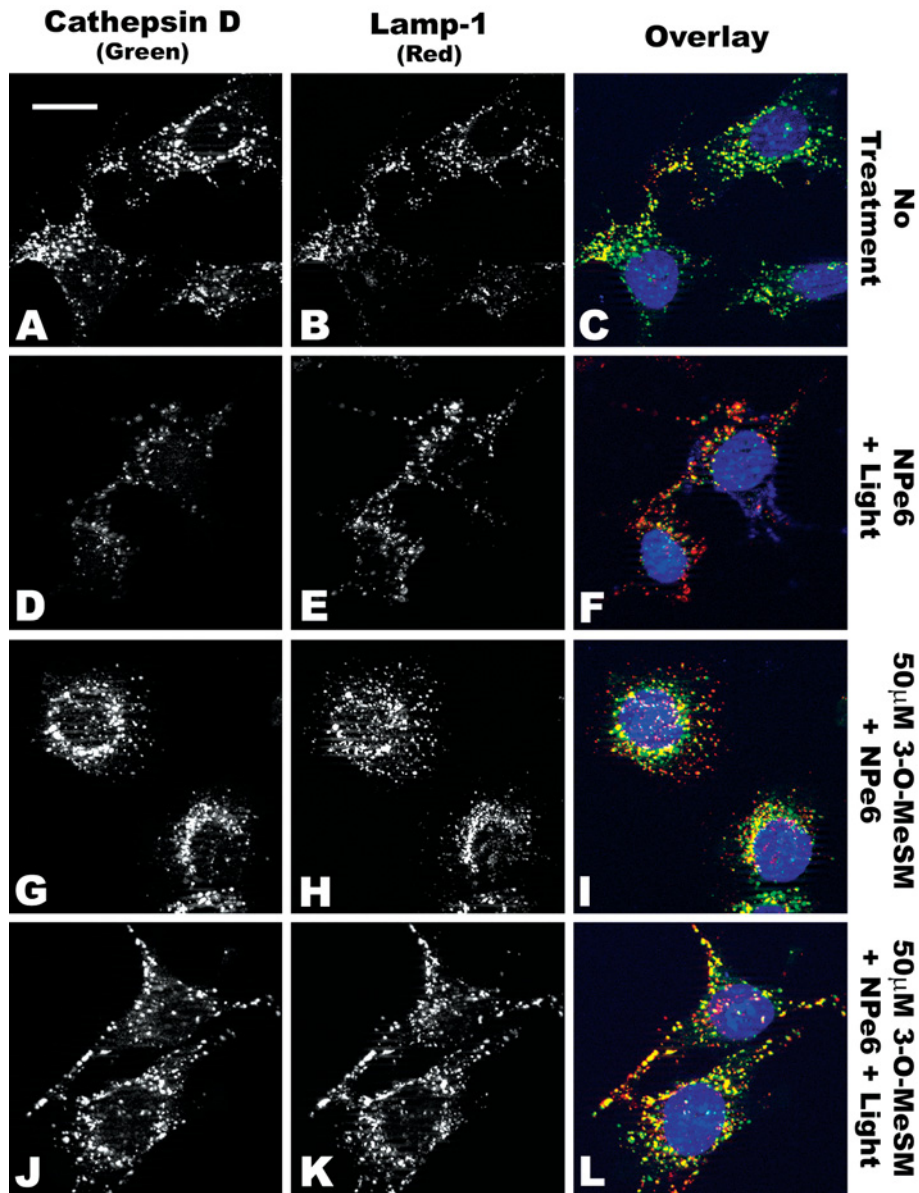
Figure 7 3-*O*-MeSM suppression of PDT-induced cathepsin D release

1c1c7 cultures grown on coverslips were left untreated (**A–C**) or treated with 33 μM NPe6 + 40 s of light (**D–F**), 33 μM NPe6 + 50 μM 3-*O*-MeSM (**G–I**) or 33 μM NPe6 + 50 μM 3-*O*-MeSM + 40 s of light (**J–L**) before being processed for analyses of cathepsin D (**A**, **D**, **G**, **J**) and Lamp-1 (**B**, **E**, **H**, **K**). Cultures were treated with NPe6 for 60 min before being washed, re-fed and irradiated. 3-*O*-MeSM was added to some cultures 30 min before irradiation. Cultures were washed and fixed for staining approx. 30 min after irradiation. Immunostained coverslips were incubated with 500 nM HO33342 for 5 min before fluorescence microscopy. All Figures were derived from comparable *z* plane scans. Exposure times and contrast adjustments were identical for (**A–L**). (**A**) Scale bar, 20 μm.

ER-associated Bcl-2 is extremely sensitive to photodamage by PDT sensitizers that target these organelles, as monitored by the loss of immunoreactivity in Western-blot assays [34–36]. The NPe6/PDT conditions used in the present study have absolutely no effect on Bcl-2 immunoreactivity in 1c1c7 cultures [34,36]. Therefore the antiapoptotic effects of 3-*O*-MeSM in our NPe6/PDT most probably reflect the sphingolipid's ability to suppress acidic organelle damage and membrane permeabilization.

Although 3-*O*-MeSM pre-treatment was protective in the NPe6/PDT, similar effects were not observed with other classes of proapoptotic inducers. Specifically, 3-*O*-MeSM either had no effect, or accelerated/potentiated apoptosis initiated by HA14-1,

staurosporine, tunicamycin and thapsigargin. HA14-1 is an effective initiator of the intrinsic apoptotic pathway. It functionally inactivates Bcl-2/Bcl-X$_L$, induces Ca^{2+} release from the ER and uncouples mitochondrial electron transport, resulting in the loss of mitochondrial membrane potential and release of cytochrome *c* [37–39]. Staurosporine is also a potent activator of the intrinsic apoptotic pathway [40]. Tunicamycin and thapsigargin are disrupters of ER/Golgi function and prototypical activators of procaspase-12 and the proapoptotic ER stress pathway [41–43]. In contrast, 3-*O*-MeSM suppressed the induction of apoptosis by TNFα over the same concentration range that was effective in the NPe6/PDT. Numerous studies have implicated acidic organelle disruption and released cathepsins in the proapoptotic mechanism
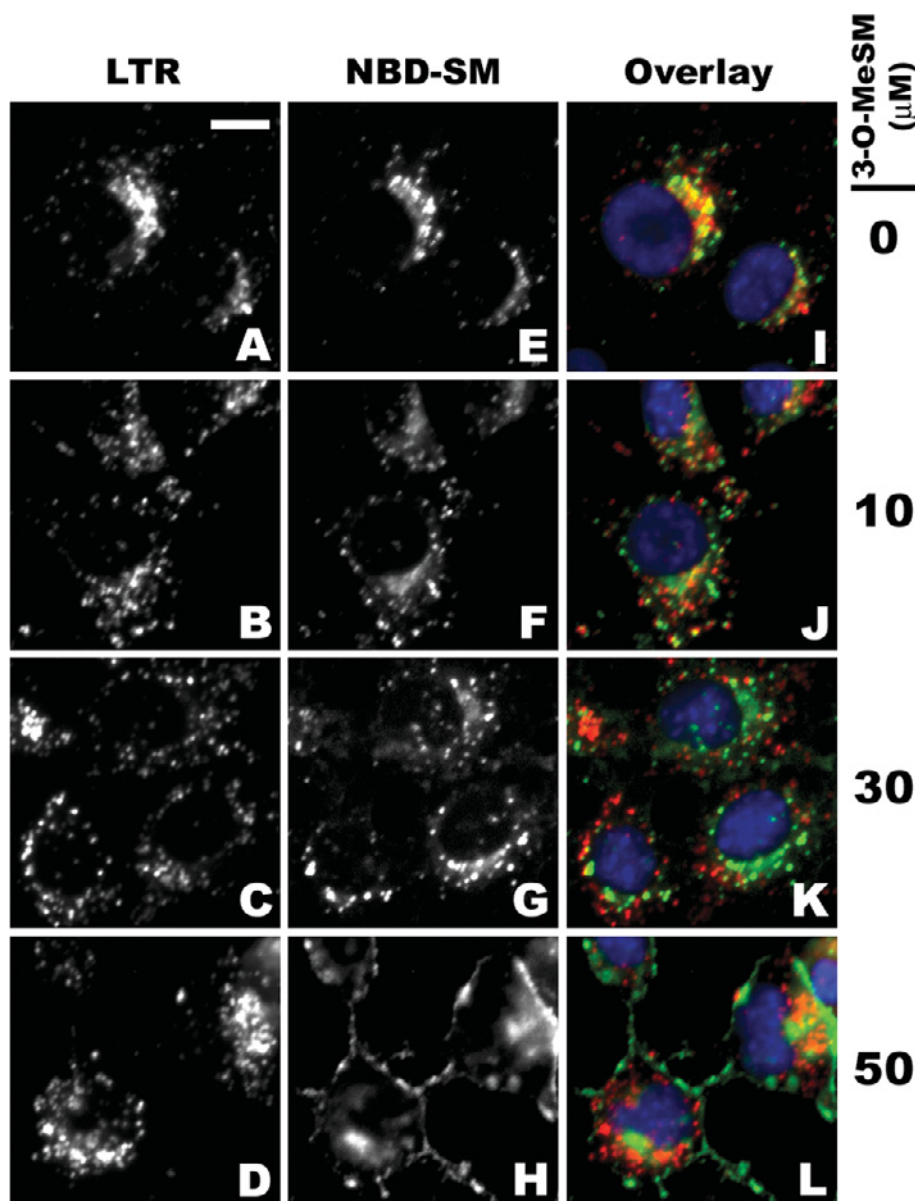
Figure 8   Competition by 3-*O*-MeSM with NBD-SM for acid organelles

1c1c7 cultures were loaded with 100 nM LTR, 5 μM NBD-SM $\pm$ various concentrations of 3-*O*-MeSM and with 500 nM HO33342 for 60, 30 and 10 min respectively before washing and fluorescence microscopy. NBD-SM and 3-*O*-MeSM were added within seconds of one another. (**A**) Scale bar, 10 μm.

of TNFα [10,13–17]. Indeed, we have preliminary data suggesting that acidic organelle disruption occurs in TNFα-treated 1c1c7 cultures by a mechanism that can be suppressed by 3-*O*-MeSM (J. A. Caruso and J. J. Reiners, Jr, unpublished work).

We do not know how 3-*O*-MeSM modulates acidic organelle fragility/permeability. However, we can eliminate two obvious possibilities. First, reduced sensitivity in our PDT protocol is not due to a suppression of NPe6 loading. Secondly, PDT-induced co-oxidation of dichlorodihydrofluorescein is similar in 1c1c7 cultures in the presence and absence of 3-*O*-MeSM (J. A. Caruso and J. J. Reiners, Jr, unpublished work). Hence, 3-*O*-MeSM is not acting as a quencher of singlet oxygen or other reactive oxygen species generated by the method.

Although unproven, we assume that 3-*O*-MeSM, like NBD-SM [31–33], is taken up by endocytosis and trafficked to early endosomes/sorting vesicles. Based on the competition of 3-*O*-MeSM with NBD-SM for co-localization with LTR (Figure 8), it appears probable that 3-*O*-MeSM is trafficked to the acidic organelle compartment within 30 min of its being added to cultures. Zager [44] reported that exogenously added SM moderately protects against oxidant-induced proximal tubule cell injury and suggested that this effect is a consequence of alterations in membrane fluidity. Membrane SMs form the scaffold for incorporation of cholesterol, and cholesterol content influences membrane fluidity [45,46]. Exogenously added SM offered some protection in our PDT model, but not as much as 3-*O*-MeSM. This difference may simply reflect differences in the solubilities of the two SMs. In our hands, 3-*O*-MeSM was clearly the more soluble of the two. Alternatively, the differential protective effects may have to do with differences at C-3. The C-3 hydroxy group on SM can function as either a hydrogen donor or a hydrogen acceptor and, along with the amide group of the sphingolipid, strongly

influences lateral interactions with adjacent SM molecules [47]. Conversion of the C-3 hydroxy group into a methoxy derivative may modify SM–SM interactions and cholesterol incorporation/packing such that the fluidity/fragility of organelle membranes is affected. Future studies are directed at examining this possibility.

A limited number of endogenous proteins have been implicated as modulators of lysosome fragility. Examples include the AhR (aryl hydrocarbon receptor) [19], cathepsin B [17], Bcl-2 [48], HSP70 (heat-shock protein 70) [49] and p53 [50]. The AhR is generally perceived as being a ligand-activated transcription factor. However, we have shown that AhR content in cells of the 1c1c7 lineage, in the absence of any exogenous ligand, modulates lysosome susceptibility to disruption by NPe6 in PDT [19]. Recent studies with the same cell lines have also shown that susceptibilities to TNFα and C$_2$-ceramide are regulated in a similar AhR content-dependent manner ([51] and J. A. Caruso and J. J. Reiners, Jr, unpublished work). Gores' laboratory has shown that TNFα-induced lysosomal protease release in hepatocytes is regulated by the lysosomal content of cathepsin B. Specifically, depletion of cathepsin B reduced both TNFα-induced lysosome disruption and hepatotoxicity [17]. In the case of Bcl-2, Brunk's laboratory used multiple approaches to demonstrate that phosphorylated Bcl-2 stabilizes lysosomes against oxidant-induced damage [48]. Similarly, the association of HSP70 with lysosomes has been reported to prevent the disruption of lysosomes by TNFα and H$_2$O$_2$ [49]. In contrast with the above cases, p53 may destabilize lysosomes. Specifically, Yuan et al. [50] recently described a study in which lysosomal destabilization and leakage occurred in a myeloid leukaemic cell line after p53 activation induced by a temperature shift. These effects occurred in the absence of any exogenous cytotoxicant. The mechanisms by which the above proteins modulate lysosomal stability/fragility are not known.

In summary, we have shown that 3-*O*-MeSM suppresses the disruption of late endosomes/lysosomes caused by a targeted oxidative stress. Given the specificity of the protective effects, 3-*O*-MeSM may be a useful tool for assessing the contributions of acidic organelle damage and protease release to the cytotoxicities of proapoptotic agents. The present study also raises the issue of whether modulation of sphingolipid content/type can influence susceptibility to specific classes of apoptotic inducers. This question may be particularly germane to diseases with perturbations of SM/cholesterol contents, such as lysosomal storage diseases [52–54].

REFERENCES

1   Eskelinen, E.-L., Tanaka, Y. and Saftig, P. (2003) At the acidic edge: emerging functions for lysosomal membrane proteins. Trends Cell Biol. **13**, 137–145

2   Mullins, C. and Bonifacino, J. S. (2001) The molecular machinery for lysosome biogenesis. BioEssays **23**, 333–343

3   Pillay, C. S., Elliott, E. and Dennison, C. (2002) Endolysosomal proteolysis and its regulation. Biochem. J. **363**, 417–429

4   Roberg, K., Johansson, U. and Öllinger, K. (1999) Lysosomal release of cathepsin D precedes relocation of cytochrome *c* and loss of mitochondrial transmembrane potential during apoptosis induced by oxidative stress. Free Radical Biol. Med. **27**, 1228–1237

5   Antunes, F., Cadenas, E. and Brunk, U. T. (2001) Apoptosis induced by exposure to a low steady-state concentration of hydrogen peroxide is a consequence of lysosomal rupture. Biochem. J. **356**, 549–555

6   Dare, E., Li, W., Zhivotovsky, B., Yuan, S. and Ceccatelli, S. (2001) Methylmercury and H$_2$O$_2$ provoke lysosomal damage in human astrocytoma D384 cells followed by apoptosis. Free Radical Biol. Med. **30**, 1347–1356

7   Öllinger, K. (2000) Inhibition of cathepsin D prevents free-radical-induced apoptosis in rat cardiomyocytes. Arch. Biochem. Biophys. **373**, 346–351

8   Reiners, Jr, J. J., Caruso, J. A., Mathieu, P., Chelladurai, B., Yin, X.-M. and Kessel, D. (2002) Release of cytochrome c and activation of pro-caspase-9 following lysosomal photodamage involves Bid cleavage. Cell Death Differ. **9**, 934–944

9   Kagedal, K., Zhao, M., Svensson, I. and Brunk, U. T. (2001) Sphingosine-induced apoptosis is dependent on lysosomal proteases. Biochem. J. **359**, 335–343

10   Werneburg, N. W., Guicciardi, M. E., Bronk, S. F. and Gores, G. J. (2002) Tumor necrosis factor-α-associated lysosomal permeabilization is cathepsin B dependent. Am. J. Physiol. Gastrointest. Liver Physiol. **283**, G947–G956

11   Neuzil, J., Zhao, M., Ostermann, G., Sticha, M., Gellert, N., Weber, C., Eaton, J. W. and Brunk, U. T. (2002) Alpha-tocopheryl succinate, an agent with *in vivo* anti-tumor activity, induces apoptosis by causing lysosomal instability. Biochem. J. **362**, 709–715

12   Ji, Z. S., Miranda, R. D., Newhouse, Y. M., Weisgraber, K. H., Huang, Y. and Mahley, R. W. (2002) Apolipoprotein E4 potentiates amyloid beta peptide-induced lysosomal leakage and apoptosis in neuronal cells. J. Biol. Chem. **277**, 21821–21828

13   Guicciardi, M. E., Deussing, J., Miyoshi, H., Bronk, S. F., Svingen, P. A., Peters, C., Kaufmann, S. H. and Gores, G. J. (2000) Cathepsin B contributes to TNF-α-mediated hepatocyte apoptosis by promoting mitochondrial release of cytochrome c. J. Clin. Invest. **106**, 1127–1137

14   Foghsgaard, L., Wissing, D., Mauch, D., Lademann, U., Bastholm, L., Boes, M., Elling, F., Leist, M. and Jäättelä, M. (2001) Cathepsin B acts as a dominant execution protease in tumor cell apoptosis induced by tumor necrosis factor. J. Cell Biol. **153**, 999–1009

15   Monney, L., Olivier, R., Otter, I., Jansen, B., Poirier, G. G. and Borner, C. (1998) Role of an acidic compartment in tumor-necrosis-factor-α-induced production of ceramide, activation of caspase-3 and apoptosis. Eur. J. Biochem. **251**, 295–303

16   Ono, K., Wang, X. and Han, J. (2001) Resistance to tumor necrosis factor-induced cell death mediated by PMCA4 deficiency. Mol. Cell. Biol. **21**, 8276–8288

17   Guicciardi, M. E., Miyoshi, H., Bronk, S. F. and Gores, G. J. (2001) Cathepsin B knockout mice are resistant to tumor necrosis factor-alpha-mediated hepatocyte apoptosis and liver injury: implications for therapeutic applications. Am. J. Pathol. **159**, 2045–2054

18   Stoka, V., Turk, B., Schendel, S. L., Kim, T.-H., Cirman, T., Snipas, S. J., Ellerby, L. M., Bredesen, D., Freeze, H., Abrahamson, M. et al. (2001) Lysosomal protease pathways to apoptosis: cleavage of Bid, not pro-caspases, is the most likely route. J. Biol. Chem. **276**, 3149–3157

19   Caruso, J. A., Mathieu, P. A., Joiakim, A., Leeson, B., Kessel, D., Sloane, B. F. and Reiners, Jr, J. J. (2004) Differential susceptibilities of murine hepatoma 1c1c7 and Tao cells to the lysosomal photosensitizer NPe6: influence of aryl hydrocarbon receptor on lysosomal fragility and protease contents. Mol. Pharmacol. **65**, 1016–1028

20   Cirman, T., Oresic, K., Mazovec, G. D., Turk, V., Reed, J. C., Meyers, R. M., Salvesen, G. S. and Turk, B. (2004) Selective disruption of lysosomes in HeLa cells triggers apoptosis mediated by cleavage of Bid by multiple papain-like lysosomal cathepsins. J. Biol. Chem. **279**, 3578–3587

21   Ségui, B., Cuvillier, O., Adam-Klages, S., Garcia, V., Malagarie-Cazenave, S., Lévêque, S., Caspar-Bauguil, S., Coudert, J., Salvayre, R., Krönke, M. et al. (2001) Involvement of FAN in TNF-induced apoptosis. J. Clin. Invest. **108**, 143–151

22   Colell, A., Morales, A., Fernandez-Ceca, J. C. and Garcia-Ruiz, C. (2002) Ceramide generated by acidic sphingomyelinase contributes to tumor necrosis factor-α-mediated apoptosis in human colon HT-29 cells through glycosphingolipids formation. FEBS Lett. **526**, 135–141

23   Luberto, C., Hassler, D. F, Signorelli, P., Okamoto, Y., Sawai, H., Boros, E., Martin, D. J., Obeid, L. M., Hannun, Y. A. and Smith, G. K. (2002) Inhibition of tumor necrosis factor-induced cell death in MCF7 by a novel inhibitor of neutral sphingomyelinase. J. Biol. Chem. **277**, 41128–41139

24   Lister, M. D., Ruan, Z. S. and Bittman, R. (1995) Interaction of sphingomyelinase with sphingomyelin analogs modified at the C-1 and C-3 positions of the sphingosine backbone. Biochim. Biophys. Acta **1256**, 25–30

25   Oleinick, N. L., Morris, R. L. and Belichenko, I. (2002) The role of apoptosis in response to photodynamic therapy: what, where, why and how. Photochem. Photobiol. Sci. **1**, 1–21

26   Kessel, D., Luo, Y., Mathieu, P. and Reiners, Jr, J. J. (2000) Determinants of the apoptotic response to lysosomal photodamage. Photochem. Photobiol. **71**, 196–200

27   Won, J.-S., Im, Y.-B., Khan, M., Singh, A. K. and Singh, I. (2004) The role of neutral sphingomyelinase produced ceramide in lipopolysaccharide-mediated expression of inducible nitric oxide synthase. J. Neurochem. **88**, 583–593

28   Albouz, S., Le Saux, F., Wenger, D., Hauw, J. J. and Baumann, N. (1986) Modifications of sphingomyelin and phosphatidylcholine metabolism by tricyclic antidepressants and phenothiazines. Life Sci. **38**, 357–363

29 Hurwitz, R., Ferlinz, K. and Sandhoff, K. (1994) The tricyclic antidepressant desipramine causes proteolytic degradation of lysosomal sphingomyelinase in human fibroblasts. Biol. Chem. Hoppe Seyler **375**, 447–450

30 Xu, J., Yeh, C. H., Chen, S., He, L., Sensi, S. L., Canzoniero, L. M., Choi, D. W. and Hsu, C. Y. (1998) Involvement of de novo ceramide biosynthesis in tumor necrosis factor-alpha/cycloheximide-induced cerebral endothelial cell death. J. Biol. Chem. **273**, 16521–16526

31 Koval, M. and Pagano, R. E. (1989) Lipid recycling between plasma membrane and intracellular compartments: transport and metabolism of fluorescent sphingomyelin analogues in cultured fibroblasts. J. Cell Biol. **108**, 2169–2181

32 Tomás, M., Durán, J. M., Lázaro-Diéguez, F., Babiá, T., Renau-Piqueras, J. and Egea, G. (2004) Fluorescent analogues of plasma membrane sphingolipids are sorted to different intracellular compartments in astrocytes. FEBS Lett. **563**, 59–65

33 Babiá, T., Ledesma, M. D., Saffrich, R., Kok, J. W., Dotti, C. G. and Egea, G. (2001) Endocytosis of NBD-sphingolipids in neurons: exclusion from degradative compartments and transport to the Golgi complex. Traffic **2**, 395–405

34 Kessel, D., Castelli, M. and Reiners, Jr, J. J. (2005) Ruthenium red-mediated suppression of Bcl-2 loss and Ca^{2+} release initiated by photodamage to the endoplasmic reticulum: scavenging of reactive oxygen species. Cell Death Differ. **12**, 502–511

35 Xue, L. Y., Chiu, S. M. and Oleinick, N. L. (2001) Photochemical destruction of the Bcl-2 oncoprotein during photodynamic therapy with the phthalocyanine photosensitizer Pc4. Oncogene **20**, 3420–3427

36 Castelli, M., Reiners, Jr, J. J. and Kessel, D. (2004) A mechanism for the pro-apoptotic activity of ursodeoxycholic acid: effects on Bcl-2 conformation. Cell Death Differ. **11**, 906–914

37 Wang, J. L., Liu, D., Zhang, Z. J., Shan, S., Han, X., Srinivasula, S. M., Croce, C. M., Alnemri, E. S. and Huang, Z. (2000) Structure-based discovery of an organic compound that binds Bcl-2 protein and induces apoptosis of tumor cells. Proc. Natl. Acad. Sci. U.S.A. **97**, 7124–7129

38 An, J., Chen, Y. and Huang, Z. (2004) Critical upstream signals of cytochrome c release induced by a novel Bcl-2 inhibitor. J. Biol. Chem. **279**, 19133–19140

39 Hao, J. H., Yu, M., Liu, F. T., Newland, A. C. and Jia, L. (2004) Bcl-2 inhibitors sensitize tumor necrosis factor-related apoptosis inducing ligand-induced apoptosis by uncoupling of mitochondrial respiration in human leukemic CEM cells. Cancer Res. **64**, 3607–3616

40 Zhang, X. D., Gillespie, S. K. and Hersey, P. (2004) Staurosporine induces apoptosis of melanoma by both caspase-dependent and -independent apoptotic pathways. Mol. Cancer Ther. **3**, 187–197

41 Rao, R. V., Hermel, E., Castro-Obregon, S., Del Rio, G., Ellerby, L. M., Ellerby, H. M. and Bredesen, D. E. (2001) Coupling endoplasmic reticulum stress to the cell death program. J. Biol. Chem. **276**, 33869–33874

42 Morishima, N., Nakanishi, K., Takenouchi, H., Shibata, T. and Yasuhiko, Y. (2002) An endoplasmic reticulum stress-specific caspase cascade in apoptosis. J. Biol. Chem. **277**, 34287–34294

43 Breckenridge, D. G., Germain, M., Mathai, J. P., Nguyen, M. and Shore, G. C. (2003) Regulation of apoptosis by endoplasmic reticulum pathways. Oncogene **22**, 8608–8618

44 Zager, R. A. (2000) Sphingomyelinase and membrane sphingomyelin content: determinants of proximal tubule cell susceptibility to injury. J. Am. Soc. Nephrol. **11**, 894–902

45 Ridway, N. D. (2000) Interactions between metabolism and intracellular distribution of cholesterol and sphingomyelin. Biochim. Biophys. Acta **1484**, 129–141

46 Simons, K. and Ikonen, E. (2000) How cells handle cholesterol. Science **290**, 1721–1726

47 Pascher, I. (1976) Molecular arrangement in sphingolipids. Biochim. Biophys. Acta **455**, 433–451

48 Zhao, M., Eaton, J. W. and Brunk, U. T. (2001) Bcl-2 phosphorylation is required for inhibition of oxidative stress-induced lysosomal leak and ensuing apoptosis. FEBS Lett. **509**, 405–412

49 Nylandsted, J., Gyrd-Hansen, M., Danielewicz, A., Fehrenbacher, N., Lademann, U., Høyer-Hansen, M., Weber, E., Multhoff, G., Rohde, M. and Jäättelä, M. (2004) Heat shock protein 70 promotes cell survival by inhibiting lysosomal membrane permeabilization. J. Exp. Med. **200**, 425–435

50 Yuan, X.-M., Li, W., Dalen, H., Lotem, J., Kama, K., Sachs, R. and Brunk, U. T. (2002) Lysosomal destabilization in p53-induced apoptosis. Proc. Natl. Acad. Sci. U.S.A. **99**, 6286–6291

51 Reiners, Jr, J. J. and Clift, R. E. (1999) Aryl hydrocarbon receptor regulation of ceramide-induced apoptosis in murine hepatoma 1c1c7 cells: a function independent of aryl hydrocarbon receptor nuclear translocator. J. Biol. Chem. **274**, 2502–2510

52 Simons, K. and Gruenberg, J. (2000) Jamming the endosomal system: lipid rafts and lysosomal storage diseases. Trends Cell Biol. **10**, 459–462

53 Harzer, K., Massenkeil, G. and Frohlich, E. (2003) Concurrent increase of cholesterol, sphingomyelin and glucosylceramide in the spleen from non-neurologic Niemann-Pick type C patients but also patients possibly affected with other lipid trafficking disorders. FEBS Lett. **537**, 177–181

54 Pagano, R. E. (2003) Endocytic trafficking of glycosphingolipids in sphingolipid storage diseases. Philos. Trans. R. Soc. London Ser. B **358**, 885–891